Monte Carlo Computer Simulation of Chain Formation from Nanoparticles

Alex Y. Sinyagin,[†] Artem Belov,[†,||] Zhioyng Tang,[†] and Nicholas A. Kotov*[,†,‡,§]

Department of Chemical Engineering, Department of Materials Science, and Department of Biomedical Engineering, University of Michigan, Ann Arbor, Michigan 48109, and Karpov Institute of Physical Chemistry (NIFHI), Moscow, 103064, Russia

Received: December 6, 2005; In Final Form: February 21, 2006

Spontaneous assembly of long chains of nanoparticles (NPs) has been experimentally observed for many different materials including nanocolloids of semiconductors, metal oxides, and metals. While the origin of dipole moment in various colloids can be different, a universal explanation of chain assembly can be provided by the hypothesis of dipole−dipole attraction of nanocolloids. In this paper, we describe the application of the Monte Carlo method for modeling of self-organization of large ensembles of NPs. As the first approximation, the Derjaguin−Landau−Verwey−Overbeek (DLVO) theory provides an adequate description of self-organization of several hundreds of NPs. Unlike microscale colloids that served as a classical model for DLVO, we used a distance-dependent media dielectric constant. The simulated chains are morphologically and geometrically similar to those observed experimentally. This establishes the fundamentally important ability of NPs to self-assemble due to their intrinsic anisotropy. Thermodynamic analysis of Monte Carlo results reveals the role of partial removal of the stabilizer shell in CdTe nanocolloids necessary for reduction of interparticle repulsion. Analysis of the field distribution around short chains demonstrates that the growth of linear agglomerates is kinetically controlled by a high activation barrier for NPs approaching from all of the directions except one end of the chain. The presented algorithm can be applied to other interparticle interactions, such as induced dipoles, which can stimulate chain formation in the absence of permanent dipole moment. It can also serve as a theoretical foundation for the understanding of the large complex superstructures forming from anisotropic and anisometric NPs. Monte Carlo simulation of nanoscale dipoles can also be extended to the interactions of NP with proteins, and related biological systems important for a variety of applications in medicine.

Introduction

The unique physical properties of low-dimensional semiconductors, such as nanoparticles (NPs) and nanowires (NWs), have attracted much attention in recent years. One side of their unique behavior is the ability to self-assemble in various 1D, 2D, and 3D superstructures.[1] NP assemblies of different complexities have been tested for a variety of nanotechnology applications including sensors, energy transformation catalysis, electronics, optical materials, and potentially many others.[2−11] Despite the widespread nature of NP aggregated structures, we know little about the forces driving their formation. Besides practical aspects of nanotechnology, the necessity to establish a clear description of interparticle forces can also be seen in the synthesis of nanocolloids. A simple method for the synthesis of NWs by means of a spontaneous assembly of stabilizer-depleted NPs was recently demonstrated for CdTe[12,13] and other nanocolloids.[14−19] This experimental observation can be a convenient tool for validation for a quantitative depiction of interparticle forces in the nanoscale.

The driving force behind the NP-to-NW self-organization process is believed to be the dipole−dipole interaction of the particles. This hypothesis has strong supporting evidence as well as numerous experimental observations in different systems.[2−12,15−24] The variety of dispersions where association of particles in chains takes place is wide: from metals,[14,17,18,25−28] and metal oxides,[15,16,29] to sulfides.[19] The media varies from water[12,16,17] or alcohol[15,18] to organic.[19−21,30] The structural genesis of the NP dipole is different for different nanocolloids. II−VI semiconductor NPs in both hexagonal (i.e., wurtzite) and cubic (i.e., zinc blende) crystal structures were experimentally found to possess significant dipole moments, which clearly shows the validity of the hypothesis.[22,24] The origin of these dipoles in the wurtzite crystal structure has been attributed to the presence of polar faces along the *c*-axis. The source of the anisotropy in zinc blende NPs was initially puzzling.[23,24] Recent calculations carried out in our group demonstrate that the truncation of ideal tetrahedral structure can lead to high dipole moments in cubic semiconductors.[31,32] Similar structural effects can give rise to intrinsic polarization in many materials in the form of nanocolloids. Moreover, the contribution of other forces such as specific affinity of stabilizers to each other observed, for instance, for some TiO_2 NPs,[16] does not exclude the presence of dipole components and is more likely to exacerbate the nonuniformity of charge distribution, and therefore, necessitates formal description of dipole interactions between nanoparticles.

The existence of a dipole moment has a profound effect on the collective behavior of the NPs. Rabani et al.[33] found that for interparticle separations ∼5 times the size of the particle,

* Corresponding author. E-mail: kotov@umich.edu.
[†] Department of Chemical Engineering, University of Michigan.
[‡] Department of Materials Science, University of Michigan.
[§] Department of Biomedical Engineering, University of Michigan.
[||] Karpov Institute of Physical Chemistry.

10.1021/jp057105e CCC: $33.50
Published on Web 03/23/2006

the dipole−dipole electrostatic interaction is by far larger than the van der Waals interactions. These lengths greatly exceed the characteristic range of possible chemical interactions and thicknesses of the stabilizing shells of the particles, which were often suspected to facilitate chain formation, and thus applicable to a variety of chemical systems, which may include other nanometer scale objects. The importance of dipole interactions can be particularly significant during the initial stages of the aggregate formation until a wide gap between them and other species or similar NPs closes up. In some way, the dipole interactions of NPs or NPs and similarly sized colloids are an intrinsic part of many different low-dimensional self-organizing systems,[25−29,34−39] and in this paper we make the first step in formalizing the dipole forces between the generic nanocolloids.

Specific attention is given here to the effects of dipole−dipole forces in relatively large NP assemblies, because a statistical component of such analysis is quite essential for the understanding of the behavior of nanoscale dispersions. A theoretical assessment of forces between separate NPs can be done in a fairly straightforward manner for 2−3 NPs. The NP-to-NW transition[12,15,40] and other processes involving spontaneous self-organization of NPs[41−44] involve millions of colloidal particles. Methods of computer simulations can provide a description of the process taking into account a large number of possible configurations of the system as well as the spontaneity and random character of individual assembly steps. Previous computer simulation of colloidal systems showed that the attractive interaction potential between colloidal macro-ions with a net dipole moment in ionic solution strongly increased at short distances and might overweight the charge−charge repulsion at relevant separations.[45−47] To estimate the degree of influence exerted by the dipole moment of the individual NPs on the patterns of NP aggregation, Monte Carlo simulations of systems consisting of a few hundred of NPs interacting in water were carried out. Two important points need to be emphasized that have fundamental importance for the further studies of NP assemblies and their self-organization processes. First, the dipole moment has, unexpectedly, a substantially stronger effect on the kinetics of the chain formation rather than on thermodynamics of the tight aggregates. The latter might have been suspected as the aligning mechanism in the dispersions; however, it is the trajectory and not the global energy minimum of how the particles approach each other that holds the key in understanding the chain formation. Second, the results of our simulations clearly indicate that the dipole−dipole interaction per se cannot lead to the formation of long chains observed experimentally for CdTe and other systems. This finding implies that other most likely short-range interparticle forces, such as van der Waals forces, also play a significant role in self-organization.

Description of the Simulation Algorithm

The purpose of this section is to outline the principles of the calculations that we undertook and to describe related assumptions and limitations. To obtain the balanced geometric configuration of the system, the canonical NVT Monte Carlo method was used as follows: at the beginning of the simulation, the particles were arranged randomly by the random number generator. During each step, the particles were either moved randomly or rotated around the *X*, *Y*, and *Z* axes. The trial displacement ζ was selected from a normal distribution over the range $-\zeta_{max} < \zeta < \zeta_{max}$. Every new arrangement of the particles was accepted or rejected according to the Metropolis criterium with the probability determined by the Boltzman distribution factor. Because the goal of the modeling was not finding the global energy minimum for the system (which would correspond to a hexagonal close-packed array of particles) but finding local minima corresponding to stable particle aggregates of various shapes, the procedure was modified to account for cluster mobility. If at any stage of the simulation an aggregate was formed, that is, the particles happened to have a center-to-center distance that was equal to their diameter (contact point), then these particles in a cluster were assigned to a group. From that moment forth, the complete group was moved and randomly rotated around the center of mass, with the relative positions of the particles in the group intact. This is a standard element of Monte Carlo modeling of large particulate systems.[48] Without it, only individual particles or dimers had any mobility in the system. The larger aggregates were effectively confined to the spot where they were formed, which contradicts the well-known attributes of reactions in liquid media. This occurs because every step in which any one of the constituents tries to move away from the group is being rejected due to strong interparticle attraction at short distances.

The grouping of the particles that come sufficiently close together is justified on the basis of chemical properties of the stabilizer-depleted NPs exemplified by CdTe chains.[13] There is a strong tendency of particles to coalesce and merge their crystal lattices[12] when the reaction is carried out at room temperature, which is the case simulated here. This tendency had been demonstrated experimentally, which was the reason of its incorporation in the simulations.

After a sufficiently large number of diffusion steps and consecutive averaging, the estimated equilibrium properties of the system were analyzed. The simulation showed that the system of 20 particles reaches the relative energy balance condition, that is, $\Delta U = |\Delta U(k) - \Delta U(k-1)| < \epsilon_o$ during $k \rightarrow \infty$ steps, where ϵ_o is a predefined constant, k is the number of Monte Carlo steps, and $\Delta U(k)$ and $\Delta U(k-1)$ are the system energies on k and $k-1$ simulation steps, after $\sim 10^5$ iterations. This method has the advantages that there are no major memory requirements and the algorithm needs no complex differentiation or integration that expedites computations.

Simple coding and debugging of Monte Carlo methods make possible the modeling of sufficiently complex systems, which are too difficult for exact methods. Instead of evaluating forces to resolve incremental atomic motions, Monte Carlo methods enforce relatively large motions on the system and determine whether the new structure is energetically feasible. The advantage of the Monte Carlo method in our case is that it allows the calculation of angle averaged dipole−dipole and charge−dipole interactions that are difficult to analyze by other methods.

Monte Carlo is frequently used in chemical research especially in the simulation of liquids because of its stochastic nature. Among the tasks related to self-organization of NPs, one can mention the simulation of nanocolloid chemical potentials and pair potentials between dipolar proteins or colloids.[45−47,49,50] Monte Carlo methods are frequently applied for treating equilibrium self-assembled structures such as self-assembled polymers and equilibrium polymerization,[51,52] electrostatically directed self-assembly,[53] assembly of bis-biotinylated DNA and streptavidin,[54] and others. At the onset of this project, these studies convinced us that one could use a similar approach to calculate the chemical potential between interacting CdTe NPs, and to obtain probable geometrical configurations of the system.

The modeling process here was carried out for two and tree-dimensional systems which consisted of up to 600 CdTe NPs with diameters $d = 1.5-5.5$ nm. Each NP was approximated by a solid sphere with a permanent dipole moment and a net

charge located at the center of the particle. The magnitude of the dipole and net charge vary during different simulation runs. In accordance with experimental data,[24] the dipole moment ranged from 0 to 400 D. The assigned particle net charge varied between 0 and 5 electrons, which are located in the center of the NP. The assumption of uniform distribution of electrons is necessary at this point to avoid overwhelmingly convoluted calculations. Additionally, there are no experimental results to benchmark the chosen nonuniform electron distribution. At a later time, the nonspherical nature of the particles should be taken into account. Also, in the future we plan to gradually introduce it in the modeling process because inhomogeneous charge distribution and preferential trapping of electrons in surface and/or other defects can potentially explain the presence of strong dipole moments in a variety of systems. At the present moment, even a simulation model that addresses a simpler case of spherical NPs and uniform charge distribution demonstrates fundamentally important results leading to a better understanding of the NP behavior in solutions.

According to the general theory of stability of colloids by Derjaguin, Landau, Verwey, and Overbeek (DLVO theory), the main forces acting between colloidal particles in solution are the electrostatic forces and the van der Waals dispersion forces.[55,56] More recent investigations concluded that other forces also play an important role in colloid stability.[57−59] The approach that takes into account these non-DLVO forces is called the extended DLVO theory (XDLVO).

Our simulation was based on the classical DLVO theory, which takes into account only the electrostatic and dispersion interactions of the NPs. This approach can be viewed as overly simplistic if one is interested in strictly quantitative description of interactions of 2−3 particles. Now we want to focus on finding approaches to describe the behavior of large particular assemblies at nanometer scales. In this respect, classical DLVO has significant advantages for our simulation needs. First, it is simple, and thus it allows us to describe systems with a larger number of particles. Second, because our primary concern is to understand the effect of NP parameters on the aggregation into specific shapes with varying degrees of linearity, we are mostly interested in the forces that could impart linear symmetry to the system. Only the electrostatic component and more specifically the charge−dipole and dipole−dipole interactions are angle-dependent and could do that. As a first approach, quadrupole interactions were not considered in the present model, although it is evident they could also play a role in NP interaction and will be included in future simulation work. Assuming that the particles are spherical and uniform, the other DLVO-XDLVO forces such as van der Waals, Lewis acid−base, and steric physical interactions become centrosymmetric. So, they have a lesser impact on the organization of NPs in linearly symmetric aggregates. This was also the reason for the exclusion in this prototypical model of the molecular treatment of the solvent from the calculations, although it is known to influence the potential of mean force between nanoparticles. Only van der Waals attractions were included in the simulation at the current stage. Similar to trapped charges, little is known presently about the homogeneity of stabilizer molecule distribution on the surface of NPs, which are responsible for Lewis acid, steric physical, and some other interactions. In one of our recent publications, it was reported that the distribution of two stabilizers on nanowires is not uniform,[60] which was also confirmed by computer simulations at the atomic scale. If this is the case for NPs as well, these findings could be included at later stages of the development of this method.

On the basis of the model for a system of charged dipolar colloids or proteins presented by Phillies[61] and Bratko et al.,[45,46] the charge and dipole fluctuations were taken to be independent and the energy of the simulated system was approximated as a sum of the pair-potentials of the Coulombic charge−charge, charge−dipole, dipole−dipole interactions, and the van der Waals interaction between all of the particles in the system taken pairwise.

$$W_{\text{total}}(r,\theta,\varphi) = W_{q-q}(r) + W_{q-\mu}(r,\theta) + W_{\mu-q}(r,\theta) + W_{\mu-\mu}(r,\theta,\varphi) + W_{\text{VanderWalls}}(r) \quad (1)$$

Here, W_{total} represents the energy required to form an aggregate of a certain shape from its constituent particles located at infinite separation, W_{q-q}, $W_{\mu-q}$, $W_{\mu-\mu}$, the energies of charge−charge, charge−dipole, and dipole−dipole interactions, respectively, r is the distance between the centers of the NPs, and θ and φ are standard angle parameters in polar coordinate system. At this point, we want to mention that the sum of all of the enumerated contributions determined the particle energy as the function of the mutual geometric configuration of the system. The pair energy arising from net charge and dipole contributions may be calculated as:[61]

$$W(r) = \frac{q_i q_j}{4\pi\epsilon_0\epsilon r_{ij}} e^{-kr_{ij}} C_0^{\,2} + 2\frac{q_i\mu_j\cos(\theta_j)}{4\pi\epsilon_0\epsilon r_{ij}^{\,2}} e^{-kr_{ij}}(1+kr_{ij})C_0C_1 + \frac{\mu_i\mu_j}{4\pi\epsilon_0\epsilon r_{ij}^{\,3}}(\cos(\theta_i)\cos(\theta_j)[2+2kr_{ij}+(kr_{ij})^2] + \sin(\theta_i)\sin(\theta_j)\cos(\phi_i-\phi_j)[1+kr_{ij}])e^{-kr_{ij}}C_1^{\,2} \quad (2)$$

where

$$C_0 = \frac{e^{ka}}{1+ka}; \quad C_1 = \frac{3e^{ka}}{[2+2ka+(ka)^2+(1+ka)/\epsilon_r]}$$

Here, ϕ_i was defined as an angle between the dipole vector $\vec{\imath}$ and the vector $\vec{r}$ connecting the centers of the NPs, $0 < \theta < 2\pi$, φ_i is the angle describing the rotation of dipole around $\vec{r}$, $0 < \varphi < \pi$, $1/k$ is the Debye screening length, ϵ_0 is the permittivity of vacuum, ϵ is the effective permittivity of the medium, a is one-half of the contact distance between two interacting particles, ϵ_r is the ratio between the relative permittivity of the medium and the relative permittivity of the colloidal particle interior, and μ_i or μ_j are the dipole moments of particles i and j. Some parameters here, such as Debye screening length, should vary with the ionic strength of the system. This variation may potentially affect the assembly properties, but to a lesser extent than the key parameter, such as the magnitude of the dipole moment. Now we want to create the basic model, which can later be fine-tuned when experimental data require it. Note that the charge neutrality of the system described here is maintained in the large scale by the compensation of the charge from large NPs by small counterions, such as OH^-, Cl^-, Na^+, Cd^{2+}, etc. Locally, for instance, in the gap between the particles, the charge neutrality is not maintained, which is taken into account by eq 2.

It is important to mention a significant difference in applying DLVO and related system of equations to nanometer scale particles as opposed to traditional micrometer-sized colloids. Our case is different because the dependence of the effective permittivity on the distance between the interacting NPs needs

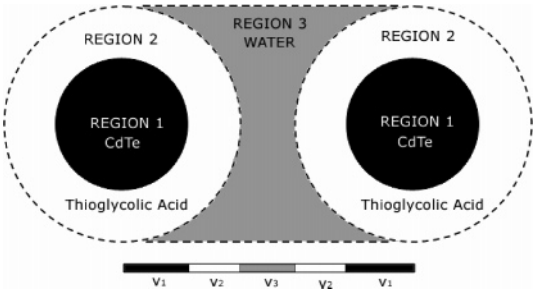

Figure 1. Schematics of the interparticle region at separations comparable to NP diameters used in the calculations of the interparticle distance dependence on the effective dielectric constant of the medium.

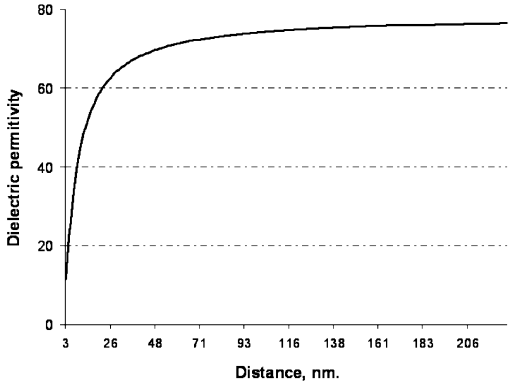

Figure 2. Dependence of effective dielectric constant of the medium on the interparticle distance calculated according to the logarithmic composite mixing rule.

to be taken into account because the thickness of the layer of stabilizer present on the NP surface is comparable to the range of r values being considered. A similar conclusion was recently made by Scott et al.[62] We used the logarithmic composite mixing rule[63] to approximate the function of ϵ on the interparticle distance r, assuming that about a monolayer of thioglycolic acid is coating the NP. Figure 1 shows the layout of the space between two interacting charges in the current model. If the charges and/or dipoles are located in the center of the NP, then the volume fraction ν of the high dielectric permittivity medium (water) decreases and so does the effective permittivity, calculated as $\log \epsilon_{\text{eff}} = \nu_1 \log \epsilon_1 + \nu_2 \log \epsilon_2 + \nu_3 \log \epsilon_3$. This approach provided an effective permittivity that ranged from nearly that of water (78.8) at large separations to just a little above that for bulk CdTe (9.96) at the point of NP contact (Figure 2).

The Hamaker molecular model of London−van der Waals forces, where the dispersion force between particles is calculated by summing the dispersion attraction between all pairs of molecules in the particles, was used in the simulation.[64] Although considerably simpler but less accurate than the molar Lifshitz approach, this model agrees well with experiments and is widely used in modeling. The van der Waals attractive energy for two equal spherical particles with the diameter d and a center-to-center separation r in this model is given as:[65]

$$W_{\text{VanderWaals}}(r) = -\frac{A_{121}}{6}\left\{\frac{d^2}{2(r^2-d^2)} + \frac{d^2}{2r^2} + \ln\left[1-\frac{d^2}{R^2}\right]\right\} \quad (3)$$

where A_{121} is the Hamaker constant for which we used the value for a closely related semiconductor CdS interacting across water, $A_{121} = 4.85 \times 10^{-20}$ J.[65] The bulk value of the Hamaker constant[66] was used in the calculation for simplicity sake, although the next step of the development of the model shall include the adjustment of the Hamaker constant for the size of the NPs. Only nonretarded interactions were taken into account because at distances where retardation becomes relevant (>5 nm) the electrostatic repulsion between similarly charged NPs outweighs the dispersion attraction.

Other relevant simulation parameters, which do not require extensive comments, are summarized in Table 1. They also represent parameters, which in perspective can be most easily varied experimentally. From the fundamental point of view, the variations of dipole moment, charge, and size (see below) seem to be the most significant. So, the relative strength of dipole−dipole, ion−dipole, ion−ion, and van der Waals interactions is being tuned in a wide range.

Simulation Results and Discussion

Finding an adequate description for incorporation of dipole−dipole interactions between the NPs in the nanoscale dynamics was our primary target in this work. Once we have a simulation model for this process, we can validate it with the existing results on the formation of NP chains. Therefore, the NP chain agglomeration process with and without dipole attraction was the starting point of our study. The simulations were carried out in two versions: two-dimensional (2D) and three-dimensional (3D) space. Because of the nature of the calculations in 3D systems, they are far more computer-time-consuming, which puts a restriction on the number of particles in the system that can be modeled on a reasonable time scale. Additionally, many important conclusions can be drawn from 2D systems and confirmed later by calculations in 3D, which is demonstrated in this paper. The first question that one can present to the simulation results is about the dependence of the geometry of NP superstructures on the dipole moment. From the theoretical point of view, it should play a decisive role in allowing chainlike structures as a result of anisotropic attraction of NPs to each other. Figure 3 shows 2D simulation results of a large ensemble of NPs with a dipole moment of either 0 or 100 D as the system moves toward thermodynamic equilibrium. Indeed, once the dipole moment is "turned on", NPs gradually agglomerate in chains, whose length is increasing with time (Figure 3A−C). At the same time, the NPs form agglomerates with random geometries (Figure 3D) when dipole moment is absent, although a similar starting distribution of NPs (Figure 3A) was used in the calculations. Thus, the presence of a dipole with a magnitude within accepted and experimentally determined limits results

TABLE 1: Summary of Simulation Parameters

simulation parameter	range	typical value
box size	[10R × 10R × 10R]−[70R × 70R × 70R]	[20R × 20R × 20R]
number of particles	10−600	50
particle diameter	2.5×10^{-9} to 6×10^{-9} m	4.4×10^{-9} m
particle charge	0 to $-5e^0$	$-1e^0$
dipole moment	0−400 D	100 D
temperature (T)	298 K	298 K

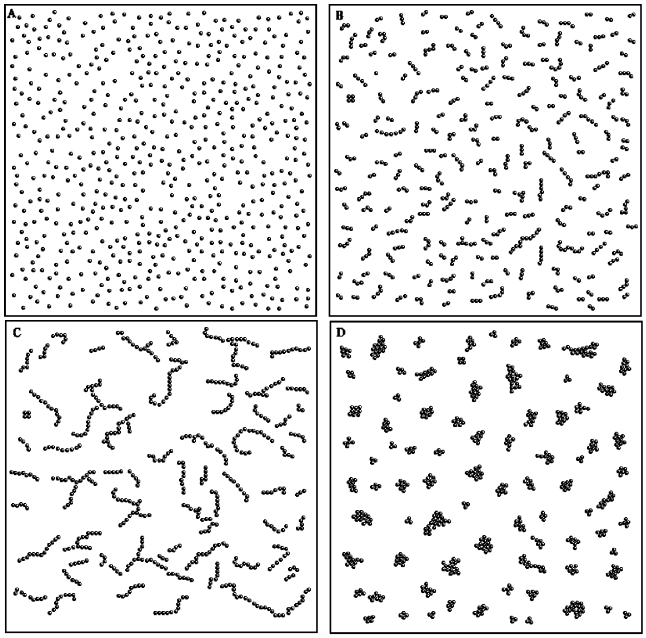

Figure 3. Results of the 2D simulation of 600 NPs with a charge of one electron and a dipole of 100 D. Starting distribution (A), intermediate (B), and final shapes (C). Same simulation with zero dipole (D).

in the formation of particle chains. This result validates the proposed simulation approach. We then can consider the role individual forces played in the process of dipole-induced self-organization, which can be elucidated from the thermodynamic analysis of the obtained NP assemblies. This is particularly useful because it can be applied to many other NP systems as well such as NP−protein mixtures, for which the spectrum of forces could be diverse. Note that dipolar particles (magnetic or electrical) could hypothetically form particle sheets in which the dipole vectors are arranged in antiparallel fashion rather than in chains. For the described system, this could happen either in case of a much higher volume content of the NPs when they are forced in multi-neighbor arrangements or when the particles have preferential axis of orientation, for instance, rods or plates.

Beside a purely visual assessment of the results, the chosen model affords calculation of the average energy of the NPs in different geometrical arrangements, which can provide an estimate of how the attractive potential is related to the favorable NP−NP orientation. The thermodynamic considerations can give us an insight into the mechanism of chain formation. Figure 4 shows the average energy per particle $\langle W \rangle = W_{\text{total}}/N$ as a function of the dipole moment for a system of 10 NPs with a diameter of 3.5 nm and different net charges arranged in a random close-packed (Figure 4A), linear (Figure 4B), and circular (Figure 4C) configuration. Several important conclusions can be made from these data:

(1) It is evident that in NP aggregates the attraction energy originating in dipole−dipole and charge−dipole forces is quite small as compared to the short-range dispersion attraction. This is quite different from the case of large separations (5 nm) considered by L. Brus and his group.[23]

(2) It can be seen that in the current model only NP with a charge lower than about five electrons could form thermodynamically stable aggregates. This fact underscores the importance of the controlled removal of the stabilizer for inducing NP self-assembly in pearl-necklace agglomerates.[12] When negatively charged thioglycolic acid is partially removed, the electrostatic repulsion can be overcome by dipole−dipole

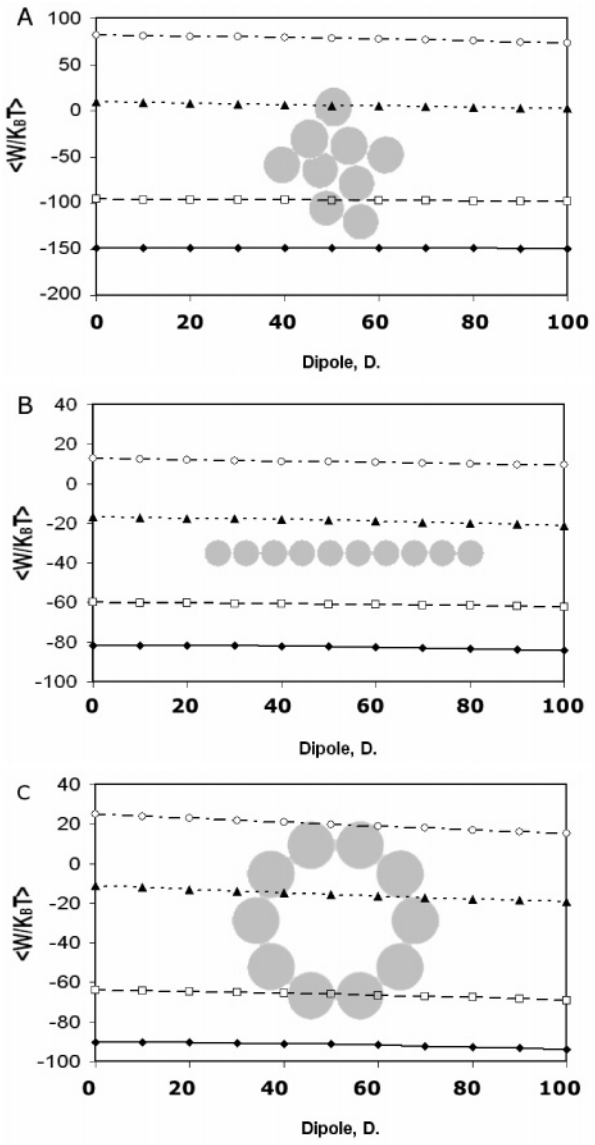

Figure 4. The average energy per particle versus dipole strength for three types of aggregates of 10 NPs ($d = 3.5$ nm) with a net charge of −1e (◆), −3e (□), −5e (▲), and −6e (O).

attraction, which can be seen as the point when the magnitude W/k_BT becomes negative.

(3) The average energy per particle for a random-shaped NP agglomerate presented in Figure 4A is much lower than that for an ordered conformation, such as chain or ring (Figure 4B,C) for low charge values. So, clumplike aggregates are substantially more favorable thermodynamically than chains. This is a fact well known from direct observations of flocculation of different kinds of colloids. For a total NP charge of five electrons (middle plot on all graphs in Figure 4), the situation changes and the electrostatic repulsion between all of the particles in the clumplike aggregate overcome the dispersion attraction, which leads to a situation where linear aggregates are still energetically favorable while random ones are not. This indicates that electrostatic repulsion plays an important role in the NP organization in chains. Therefore, fine-tuning of the NP charge offers a convenient tool for controlling the tendency of nanocolloids to agglomerate in chains. It can also hold the key to understanding many examples of pearl-necklace agglomerates in the literature.[12,17−19]

From Figure 4, one can also deduce that dipole−dipole interactions are essential but they cannot explain the experi-

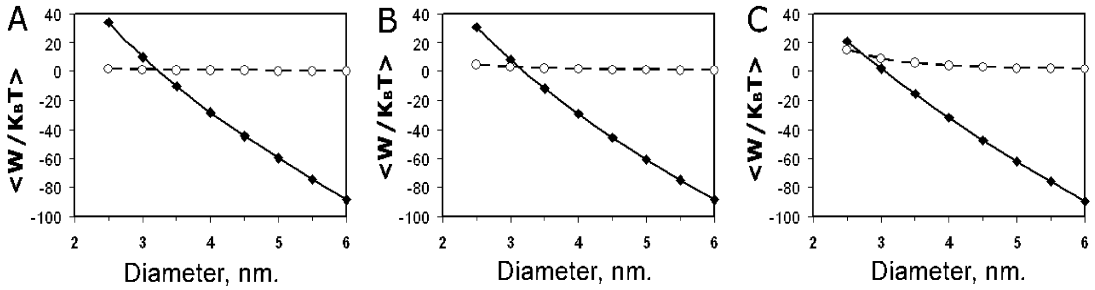

Figure 5. Average energy per particle $\langle W \rangle$ (◆) and dipole interaction energy $\langle W_{dipole} \rangle$ (O) in a linear chain of 10 NP for dipoles of 20 D (A), 50 D (B), and 100 D (C) for particle sizes 2.5−6 nm.

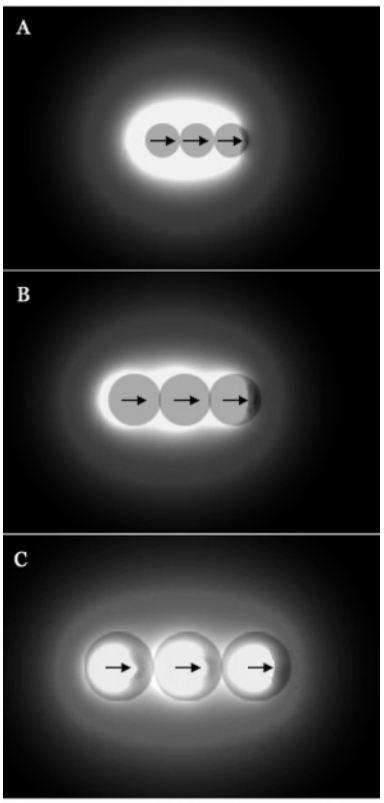

Figure 6. Distribution of electric field potential around NPs of different sizes. The net charge and dipole are constant for the three sizes. The actual sizes are arbitrary and are provided only for the visualization of the difference in the field distribution between equal dipoles at different separations.

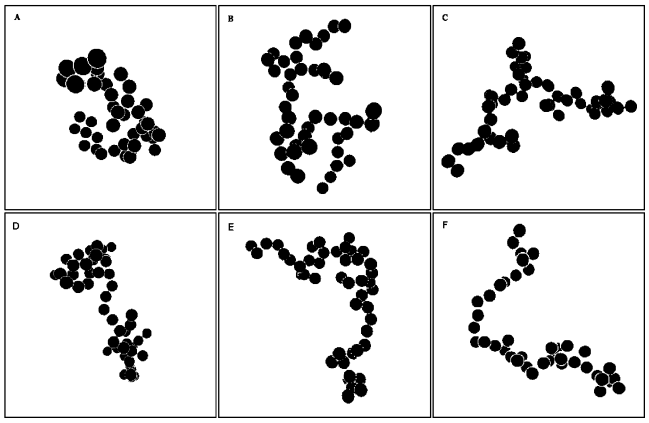

Figure 7. Results of three-dimensional simulations of nanoparticle aggregation for NPs with a diameter of 5.5 nm and a dipole moment of 25 D (A), 100 D (B), and 400 D (C) and for NPs with a diameter of 2.5 nm and a dipole moment of 25 D (D), 100 D (E), and 400 D (F). Visual differences in particle diameters represent their 3D position along the axis perpendicular to the plane of image.

mental NP assembly results without the contributions of other forces. This important conclusion is relevant for further experimental work on this kind of processes, although it can hardly be arrived at on the basis of existing experimental data in this field.[12,15−19]

It is also interesting to trace the effect of particle size on the average energy per particle and the dipole−dipole contribution to the total average energy per particle $\langle W_{dipole} \rangle = \langle W_{currentdipole} \rangle - \langle W_{zerodipole} \rangle$ for three increasing dipole values (Figure 5). The energy of the smaller particles shows a greater dependence on the magnitude of the dipole. This happens because as the size gets smaller, the contribution of the electrostatic component to the total particle energy increases.

Let us now try to understand the role of the permanent dipole in the self-organization of the NPs in chains. On one hand, we know from the experiments that its presence is exceptionally essential for self-organization to occur. On the other hand, the energy of the dipole attraction seems to be insignificant from the point of view of holding together aggregates of definite shapes (Figure 4) because the nondirectional van der Waals attraction makes a substantially greater contribution in the energy of NP assemblies at small separations. Additionally, the thermodynamics of random agglomerates seems to be a lot more favorable for the majority of NP dispersions. Thus, how can dipole−dipole interactions govern the aggregation of NPs into chainlike as opposed to clumplike structures? The answer to this question comes from the study of the distribution of the potential of the electric field around the nanoparticles (Figure 6). Here, three trimers of different sized NPs with the same net charge and dipole moment are presented overlaid on the field potential. It can be seen that if another similarly charged and polar particle would approach the chain, the gradient of the field would be the smallest along the long axis of the trimer from the side of the opposite charged end of the dipole. This can be best seen for the smallest particles where only the rightmost one is accessible without bumping into the high potential area (coded as white color in Figure 6).

So, it can be assumed that the formation of chainlike structures proceeds in the solution by a step-by-step process where either chains grow by sweeping individual particles or dimers as they diffuse in the solution, approaching them with the "right" side, or small chain fragments of 2 to maybe 4 constituents are formed from the individual NPs and then bind together to form large aggregates. Of course during the diffusion in a real solution occasionally two chains or fragments would overcome the potential barrier on the "wrong" side and come within the area where the dispersion attraction prevails upon the electrostatic repulsion, in which case they would be stuck in a "dipole-unfavorable" conformation. This is the mechanism by which branching, chain doubling, and other chain defects

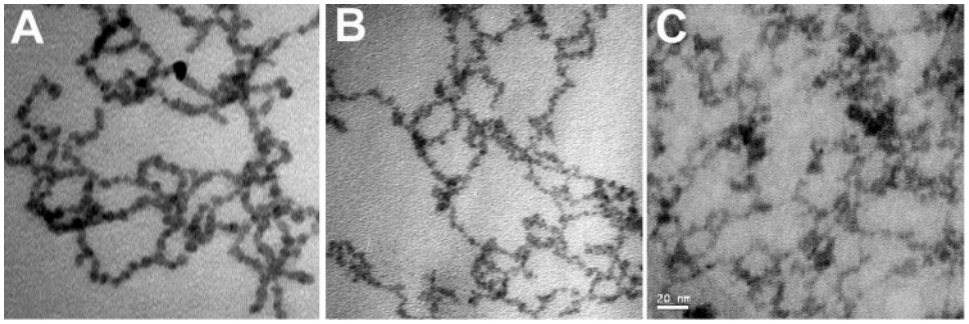

Figure 8. TEM image of NP chains forming during the NP→NW transition of CdTe colloids with a diameter of 5.4 ± 0.4 nm (A), 3.4 ± 0.3 nm (B), and 2.5 ± 0.3 nm (C).

would occur, and the elaborate pearl-necklace shapes could arise. The data from Figures 3 and 4 on the size dependence of the electrostatic component of the particle interaction enable us to suppose that aggregates of smaller NPs should be more linear and have less branching and defects (Figure 6A) than aggregates of larger particles for which the potential barrier is more uniform on all sides (Figure 6C).

To test these considerations made for the 2D system, our 3D simulation program was modified to accommodate the movement and rotation of whole groups of aggregated particles as single entities. As described in the simulation details section, as soon as particles approached to a minimal distance of each other they were considered a group and handled together. This approach allowed us to approximately simulate the movement of oligomers in solution, because the system would favor an orientation, which would minimize interaction energy with neighboring oligomers (the "right" orientation). Results from three-dimensional simulations are presented in Figure 7. As can be seen, the visible degree of linearity is again strongly dependent on the size of the dipole (compare Figure 7A vs C and Figure 7D vs F). The actual shape of the aggregates seems to support the finding about the strong anisotropy of electrical field around the NP oligomers (Figure 6).

The particle size also affects the geometry of the chains. The visual linearity of aggregates of 2.5 nm is higher than that for 5.5 nm NPs (compare, for instance, Figure 7C vs F). Thus, being under identical conditions and bearing equal dipole moments, smaller NPs make more linear aggregates.

It is interesting to compare the calculated and experimental geometries of the chains. First, pearl-necklace aggregates in the TEM images (Figure 8) appear to closely resemble the chains in Figures 3 and 7. According to literature data, CdTe NPs in Figure 8 should have the dipole moment around 100 D.[22−24] More accurate experimental data are difficult to obtain because the removal of stabilizer (thioglycolic acid) may result in spontaneous switching of crystal lattice packing from cubic to hexagonal, which should have drastically different lattice polarization and thus the dipole moment. Assuming that the magnitude of the actual dipole is indeed close to 100 D (which is close to experimental and calculated data), the comparison of Figure 7B,E and Figure 8 becomes even more obvious. This demonstrates that the theory of the force fields around NPs used here does describe the inter-NP interactions quite well.

With respect to the degree of linearity and density of branching points, which is predicted to depend on particle size, one can compare Figure 8A and Figure 8B obtained for CdTe colloids with a diameter of 5.4 ± 0.5 and 3.4 ± 0.3 nm, respectively. Visual assessment of these representative TEMs does indicate that the particle chains from smaller NPs have a lower tendency of branching. When we go, however, to even smaller particles with a diameter of 2.5 ± 0.3 nm (Figure 8C), the situation changes drastically and chains appear to be more convoluted. The reason for this is the dependence of the dipole molecule on NP size. Unfortunately, one cannot make experimentally colloids of different diameters bearing equal dipoles. The significant decrease of degree of linearity in Figure 8C is related to the drastic drop in the magnitude of the dipole moment. Therefore, the chains in Figure 8C should be more likely compared to their theoretical counterparts in Figure 7D calculated for 25 D dipole. Considering that TEM gives a 2D projection of the 3D chain, the calculated and experimental images are alike.

We also want to mention an important discrepancy between the simulation results in both 2D and 3D and the experimental TEM pictures. Linear, single-particle chains comprised of dozens of NPs are routinely observed on photographs (Figure 8A), whereas they are unable to form in any of the simulations carried out so far. Increasing the dipole moments to high magnitudes such as 400 D only marginally extends the chain length. This suggests that simple dipole−dipole and dipole−charge interactions are not sufficient for the full description of the NP interactions. Additional strong short-range forces that can hold together the formed chain intact and long-distance attractive forces that can direct the attachment of new particles and extend the average length of the chains should also be taken into account in more advanced models. Establishing the nature of these forces will be important for understanding and controlling the structure of NP superstructures of various types.

Conclusion

Monte Carlo simulations of systems of interacting NPs demonstrated that the presence of a dipole moment on the NP could lead them to assemble into structures with a varying degree of linearity. The proposed theoretical treatment allowed one for the first time to untangle the interplay of electrostatic repulsion, dipole attraction, and dispersion forces in NP dispersions. Comparison with previously obtained experimental data firmly validates the described simulation model. Thermodynamic analysis of the assembly process established the importance and role of partial removal of the stabilizer shell around the nanocrystalline colloid. It is necessary for reduction of the overall charges that makes the formation of the linear aggregates an energetically favorable process. The calculated 3D images closely resemble the experimental TEMs of CdTe pearl-necklace aggregates. This fact indicates the applicability of the suggested force field parameters for the description of inter-NP interactions. However, the current model cannot account for the formation of experimentally observable NP chains of high length, thus suggesting that additional forces and interactions should be taken into account when modeling NP systems. Some of those interactions could include induced dipoles, higher

multipoles, and hydrophobic and other short-range forces. The proposed description of the force field including the dependence of dielectric constant on interparticle distance and the simulation algorithm can be applied to other systems, for example, the interactions of NPs and proteins, viruses, micelles, and vesicles relevant for biomedical applications of nanoparticles.

References and Notes

(1) Kotov, N. A.; Tang, Z. Y. *Nanoparticle Assemblies and Superstructures*; Taylor & Francis Group: 2005; pp 1−626.

(2) Boal, A. K.; Frankamp, B. L.; Usun, O.; Tuominen, M. T.; Rotello, V. *Chem. Mater.* **2004**, *16*, 3252−3256.

(3) Boeker, A.; Lin, Y.; Chiapperini, K.; Horowitz, R.; Thompson, M.; Carreon, V.; Xu, T.; Abetz, C.; Skaff, H.; Dinsmore, A. D.; Emrick, T.; Russell, T. P. *Nat. Mater.* **2004**, *3*, 302−306.

(4) Cheng, W.; Jiang, J.; Dong, S.; Wang, E. *Chem. Commun.* **2002**, *16*, 1706−1707.

(5) Claridge, S. A.; Goh, S. L.; Frechet, J.-M. J.; Williams, S. C.; Micheel, C. M.; Alivisatos, A. P. *Chem. Mater.* **2005**, *17*, 1628−1635.

(6) Kiely, C. J. *Faraday Discuss.* **2004**, *125*, 409−414.

(7) Maye, M. M.; Lim, I.-I. S.; Luo, J.; Rab, Z.; Rabinovich, D.; Liu, T.; Zhong, C.-J. *J. Am. Chem. Soc.* **2005**, *127*, 1519−1529.

(8) Murphy, C. *J. Mol. Supramol. Photochem.* **2000**, *6*, 285−309.

(9) Roth, C.; Hussain, I.; Bayati, M.; Nichols, R. J.; Schiffrin, D. *J. Chem. Commun.* **2004**, *13*, 1532−1533.

(10) Tang, Z.; Kotov, N. A. *Adv. Mater.* **2005**, *17*, 951−962.

(11) Willner, I.; Willner, B. *Pure Appl. Chem.* **2002**, *74*, 1773−1783.

(12) Tang, Z. Y.; Kotov, N. A.; Giersig, M. *Science* **2002**, *297*, 237−240.

(13) Tang, Z. Y.; Ozturk, B.; Wang, Y.; Kotov, N. A. *J. Phys. Chem. B* **2004**, *108*, 6927−6931.

(14) Korgel, B. A.; Fitzmaurice, D. *Adv. Mater.* **1998**, *10*, 661−665.

(15) Pacholski, C.; Kornowski, A.; Weller, H. *Angew. Chem., Int. Ed.* **2002**, *41*, 1188−1191.

(16) Polleux, J.; Pinna, N.; Antonietti, M.; Niederberger, M. *Adv. Mater.* **2004**, *16*, 436−439.

(17) Chang, J. Y.; Chang, J. J.; Lo, B.; Tzing, S. H.; Ling, Y. C. *Chem. Phys. Lett.* **2003**, *379*, 261−267.

(18) Liao, J. H.; Zhang, Y.; Yu, W.; Xu, L. N.; Ge, C. W.; Liu, J. H.; Gu, N. *Colloids Surf., A* **2003**, *223*, 177−183.

(19) Gao, F.; Lu, Q. Y.; Zhao, D. Y. *Nano Lett.* **2003**, *3*, 85−88.

(20) Kan, S.; Mokari, T.; Rothenberg, E.; Banin, U. *Nat. Mater.* **2003**, *2*, 155−158.

(21) Yin, M.; Gu, Y.; Kuskovsky, I. L.; Andelman, T.; Zhu, Y.; Neumark, G. F.; O'Brien, S. *J. Am. Chem. Soc.* **2004**, *126*, 6206−6207.

(22) Blanton, S. A.; Leheny, R. L.; Hines, M. A.; GuyotSionnest, P. *Phys. Rev. Lett.* **1997**, *79*, 865−868.

(23) Rabani, E. *J. Chem. Phys.* **2001**, *115*, 1493−1497.

(24) Shim, M.; Guyot-Sionnest, P. *J. Chem. Phys.* **1999**, *111*, 6955−6964.

(25) Dai, Q.; Worden, J. G.; Trullinger, J.; Huo, Q. A. *J. Am. Chem. Soc.* **2005**, *127*, 8008−8009.

(26) Kim, G.-M.; Wutzler, A.; Radusch, H.-J.; Michler, G. H.; Simon, P.; Sperling, R. A.; Parak, W. J. *Chem. Mater.* **2005** *17*, 4949−4957.

(27) Sioss, J. A.; Keating, C. D. *Nano Lett.* **2005**, *5*, 1779−1783.

(28) Wei, Q.-H.; Su, K. H.; Durant, S.; Zhang, X. *Nano Lett.* **2005**, *4*, 1067−1071.

(29) Zhang, R.-S.; Du, F.-L. *Qingdao Daxue Xuebao, Ziran Kexueban* **2004**, *25*, 149−152.

(30) Thoma, S. G.; Sanchez, A.; Provencio, P.; Abrams, B. L.; Wilcoxon, J. P. *J. Am. Chem. Soc.* **2005**, *127*, 7611−7614.

(31) Shanbhag, S.; Kotov, N. A., in preparation.

(32) Tang, Z.; Zhang, Z. L.; Glotzer, S. C.; Kotov, N. A., in preparation.

(33) Rabani, E.; Hetenyi, B.; Berne, B. J.; Brus, L. E. *J. Chem. Phys.* **1999**, *110*, 5355−5369.

(34) Ulrich, S.; Laguecir, A.; Stoll, S. *J. Nanopart. Res.* **2004**, *6*, 595−603.

(35) Dittmer, W. U.; Simmel, F. C. *Appl. Phys. Lett.* **2004**, *85*, 633−635.

(36) Rana, N.; Yau, S.-T. *Nanotechnology* **2004**, *15*, 275−278.

(37) Sun, X. H.; Wong, N. B.; Li, C. P.; Lee, S. T.; Sham, T. K. *J. Appl. Phys.* **2004**, *96*, 3447−3451.

(38) Shenhar, R.; Rotello, V. *Acc. Chem. Res.* **2003**, *36*, 549−561.

(39) Wooley, K. L.; Hawker, C. J. *Top. Curr. Chem.* **2005**, *245*, 287−305.

(40) Cho, K. S.; Gaschler, W. L.; Murray, C. B.; Stokes, K. L. *Abstr. Pap.-Am. Chem. Soc.* **2002**, *224*, U308.

(41) Cha, J. N.; Birkedal, H.; Euliss, L. E.; Bartl, M. H.; Wong, M. S.; Deming, T. J.; Stucky, G. D. *J. Am. Chem. Soc.* **2003**, *125*, 8285−8289.

(42) Euliss, L. E.; Grancharov, S. G.; O'Brien, S.; Deming, T. J.; Stucky, G. D.; Murray, C. B.; Held, G. A. *Nano Lett.* **2003**, *3*, 1489−1493.

(43) Murthy, V. S.; Cha, J. N.; Stucky, G. D.; Wong, M. S. *J. Am. Chem. Soc.* **2004**, *126*, 5292−5299.

(44) Wong, M. S.; Cha, J. N.; Choi, K. S.; Deming, T. J.; Stucky, G. D. *Nano Lett.* **2002**, *2*, 583−587.

(45) Bratko, D.; Striolo, A.; Wu, J. Z.; Blanch, H. W.; Prausnitz, J. M. *J. Phys. Chem. B* **2002**, *106*, 2714−2720.

(46) Striolo, A.; Bratko, D.; Wu, J. Z.; Elvassore, N.; Blanch, H. W.; Prausnitz, J. M. *J. Chem. Phys.* **2002**, *116*, 7733−7743.

(47) Wu, J. Z.; Bratko, D.; Blanch, H. W.; Prausnitz, J. M. *J. Chem. Phys.* **1999**, *111*, 7084−7094.

(48) Davis, S. W.; McCausland, W.; McGahagan, H. C.; Tanaka, C. T.; Widom, M. *Phys. Rev. E* **1999**, *59*, 2424−2428.

(49) Allen, M. P.; Tildesley, D. J. *Computer Simulation of Liquids*; Clarendon Press: Oxford Oxfordshire, 1987.

(50) Tej, M. K.; Meredith, J. C. *J. Chem. Phys.* **2002**, *117*, 5443−5451.

(51) Lu, X. J.; Kindt, J. T. *J. Chem. Phys.* **2004**, *120*, 10328−10338.

(52) Wittmer, J. P.; Milchev, A.; Cates, M. E. *J. Chem. Phys.* **1998**, *109*, 834−845.

(53) Tsonchev, S.; Schatz, G. C.; Ratner, M. A. *J. Phys. Chem. B* **2004**, *108*, 8817−8822.

(54) Richter, J.; Adler, M.; Niemeyer, C. M. *ChemPhysChem* **2003**, *4*, 79−83.

(55) Derjaguin, B.; Landau, L. *Zh. Eksp. Teor. Fiz.* **1945**, *15*, 663−682.

(56) Verwey, E. J. W.; Overbeek, J. T.; Nes, K. v. *Theory of the Stability of Lyophobic Colloids the Interaction of Sol Particles Having an Electric Double Layer*; Elsevier Pub. Co: New York, 1948.

(57) Wu, W.; Giese, R. F.; van Oss, C. J. *Colloids Surf., B* **1999**, *14*, 47−55.

(58) Leckband, D.; Sivasankar, S. *Colloids Surf., B* **1999**, *14*, 83−97.

(59) Molina-Bolivar, J. A.; Ortega-Vinuesa, J. L. *Langmuir* **1999**, *15*, 2644−2653.

(60) Wang, Y.; Tang, T.; Liang, X.; Liz-Marzan, L. M.; Kotov, N. A. *Nano Lett.* **2004**, *4*, 225−231.

(61) Phillies, G. D. *J. Chem. Phys.* **1974**, *60*, 2721−2731.

(62) Scott, R.; Boland, M.; Rogale, K.; Fernandez, A. *J. Phys. A: Math. Gen.* **2004**, *37*, 9791−9803.

(63) Habeger, C. F.; Condon, C. E.; Khan, S. R.; Adair, J. H. *Colloids Surf., A* **1997**, *10*, 13−21.

(64) Hamaker, H. C. *Physica (Utrecht)* **1937**, *4*, 1058−1072.

(65) Morrison, I. D.; Ross, S. *Colloidal Dispersions, Suspensions, Emulsions and Foams*; Wiley-Interscience: New York, 2002.

(66) Lifshitz, E. M. *Sov. Phys. JETP* **1956**, *2*, 73−83.